



Swansea University
Prifysgol Abertawe



Cronfa - Swansea University Open Access Repository

This is an author produced version of a paper published in:
Crystal Growth & Design

Cronfa URL for this paper:

<http://cronfa.swan.ac.uk/Record/cronfa39418>

Paper:

Guerri, A., Taddei, M., Bataille, T., Moneti, S., Boulon, M., Sangregorio, C., Costantino, F. & Ienco, A. (2018). Same Not the Same: Thermally Driven Transformation of Nickel Phosphinate-Bipyridine One-Dimensional Chains into Three-Dimensional Coordination Polymers. *Crystal Growth & Design*, 18(4), 2234-2242.
<http://dx.doi.org/10.1021/acs.cgd.7b01672>

This item is brought to you by Swansea University. Any person downloading material is agreeing to abide by the terms of the repository licence. Copies of full text items may be used or reproduced in any format or medium, without prior permission for personal research or study, educational or non-commercial purposes only. The copyright for any work remains with the original author unless otherwise specified. The full-text must not be sold in any format or medium without the formal permission of the copyright holder.

Permission for multiple reproductions should be obtained from the original author.

Authors are personally responsible for adhering to copyright and publisher restrictions when uploading content to the repository.

<http://www.swansea.ac.uk/library/researchsupport/ris-support/>

Same not the Same: Thermally-Driven Transformation of Nickel Phosphinate-Bipyridine 1D Chains into 3D Coordination Polymers

Annalisa Guerri[§], Marco Taddei[‡], Thierry Bataille[†], Simonetta Moneti[‡], Ferdinando Costantino^{‡, †*} and Andrea Ienco^{‡*}

[§] Dipartimento di Chimica, University of Florence, Via della Lastruccia 3, I-50019, Sesto Fiorentino, Firenze, Italy

[‡] Energy Safety Research Institute, Swansea University – Bay Campus, Fabian Way, Swansea, SA1 8EN, United Kingdom

[†] Sciences Chimiques de Rennes (UMR 6226), CNRS, Université de Rennes 1, Avenue du General Leclerc, 35042 Rennes Cedex, France

[‡] Consiglio Nazionale delle Ricerche - Istituto di Chimica dei Composti Organo Metallici (CNR-ICCOM) Via Madonna del Piano 10, I-50019 Sesto Fiorentino (Firenze) Italy.

[‡] Department of Chemistry, Biology and Biotechnologies, University of Perugia, Via Elce di Sotto, 8-06124, Perugia, Italy.

Keywords: Coordination polymers, Metal phosphinates, Phase transitions, Non-ambient diffraction

ABSTRACT

Three 1D nickel coordination polymers (CPs) based on P,P'-diphenylethylenediphosphinic acid and three different bis-pyridine co-ligands, namely 4,4'-bipyridine (bipy), 1,2-bis(4-pyridyl)ethane (bpy-ane) and 1,2-bis(4-pyridyl)ethane (bpy-ene), were prepared in mild hydrothermal conditions from water solutions containing the dissolved reagents. The CPs have formula $[\text{Ni}(\text{H}_2\text{O})_4(\text{bipy})\cdot\text{pc}_2\text{p}]_n$ (**1**), $[\text{Ni}(\text{H}_2\text{O})_4(\text{bpy-ane})\cdot\text{pc}_2\text{p}]_n$ (**2**), and $[\text{Ni}(\text{H}_2\text{O})_4(\text{bpy-ene})\cdot\text{pc}_2\text{p}]_n$ (**3**) and their structures were characterized by single crystal X-ray diffraction. They are constituted of infinite $\text{Ni}(\text{H}_2\text{O})_4(\text{bis-pyridine})$ 1D rows connected, through hydrogen bonds, with the phosphinic acids placed among adjacent rows. Although the formulas and the structural topologies of the three compounds are almost identical, they behave in different manners upon heating. Compound **1** yields an amorphous phase when water molecules are thermally removed, whereas compound **3** undergoes interesting phase transformations derived from the connection of Ni atoms with the phosphinates oxygen atoms, increasing the dimensionality to 3D and maintaining crystallinity. The behavior of compound **2** has some analogies to that of **3** although a complete structural characterization was not performed because of a significant crystallinity loss of the heated phase. The structural features were studied by means of combination of variable temperature (VT) single crystal and powder X-ray diffraction and thermogravimetric analysis.

The reason for these different behaviors was ascribed to both the length and the flexibility degree of the nitrogenated co-ligands.

INTRODUCTION

Chemistry is about transformations. The large majority of chemical reactions are carried out in liquid media, being the molecules free of moving around and to assume conformations favorable to the reactions to take place.¹ Metal-organic frameworks (MOFs), and coordination polymers (CPs) in general, are classes of compounds that can easily show structural transformations at the solid state driven by external stimuli, such as light, pressure and heat.²⁻⁴ The majority of the structural changes can be ascribed either to a modification of ligand conformation or to the removal of solvent molecules, usually placed in voids or in channels as crystallization solvent. Less frequently, the formation or breakage of some bonds are also events taking place upon external stimuli and they can occur through crystal-to-crystal or crystal-to-amorphous phase transformations. Understanding the factors that influence the structural transformations in these classes of solids is crucial to gain the ability to design new and more efficient materials.⁵ Crystal-to-crystal transformation induced by the loss of crystallization water or other solvents is a typical reaction already observed in several compounds.⁶⁻⁸ However, the majority of CPs or MOFs described in the literature exhibits reversible solvent loss and/or uptake, without changes in dimensionality: in other words, no strong bonds which increase the dimensionality are formed upon solvent loss. The reversibility of this event in flexible CPs, associated with structural transformation due to changes in ligand conformation, is typically called breathing effect. A large number of MOFs and CPs reported in literature shows this phenomenon.⁹⁻¹²

The description of the transformation of a weak bond in a strong one maintaining the crystallinity of the system and changing the dimensionality of the system are still very rare to the best of our knowledge.¹³ On the contrary, CPs based on diphosphate ligands (see chart 1) frequently show structural modifications induced by the temperature, leading also to changes of the dimensionality of the network.¹⁴⁻¹⁶ Diphosphate linkers feature some chemical and geometrical similarities with carboxylate and phosphonate moieties (see chart 2). Diphosphates have the advantage of being versatile in tuning the electronic and steric properties of the organic residues attached to the phosphorus atom.

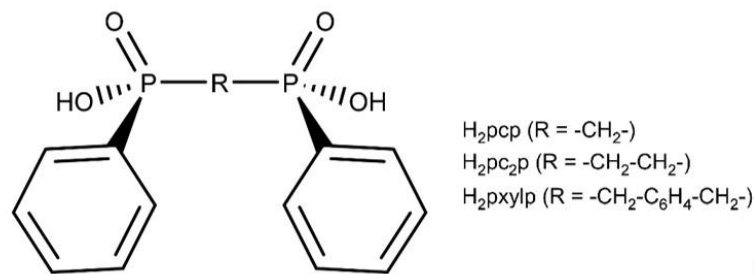


Chart 1. Molecular structure of a diphenyl-bisphosphinate with different substituting groups.

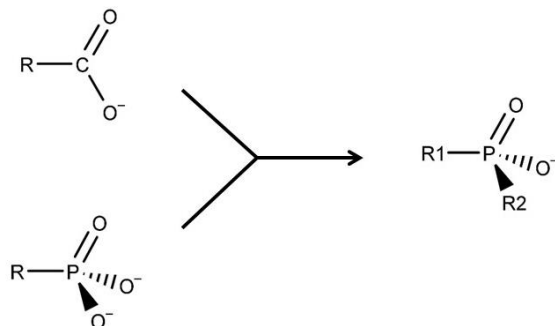


Chart 2. Structural relationships among carboxylates, phosphonates and phosphinates.

As an example, the 3D network $[\text{Cu}(\text{pc}_2\text{p})(\text{bipy})(\text{H}_2\text{O}) \cdot 2.5\text{H}_2\text{O}]_n$ (where $\text{H}_2\text{pc}_2\text{p} = \text{P},\text{P}'$ -diphenylethylenediphosphinic acid, $\text{bipy} = 4,4'$ -bipyridine) converted in different crystalline phases when heated up to 120°C . Differently, in solution, it transformed into a 2D grid $[\text{Cu}(\text{pc}_2\text{p})(\text{bipy})(\text{H}_2\text{O}) \cdot 3\text{H}_2\text{O}]_n$, showing a rare example of modification from 3D to 2D network.¹⁷ Moreover, by heating the iso-topological 2D grid $[\text{Cu}(\text{pxylp})(\text{bipy})(\text{H}_2\text{O})_2 \cdot 2\text{H}_2\text{O}]_n$ (where $\text{H}_2\text{pxylp} = \text{P},\text{P}'$ -diphenyl-*p*-xylylenediphosphinic acid), the 3D network $[\text{Cu}(\text{pxylp})(\text{bipy})]_n$ was obtained.¹⁸ Finally, the metal-organic nanotubes (MONTs) having formula $[\text{Cu}(\text{pcp})(\text{bipy}) \cdot 5\text{H}_2\text{O}]_n$ and $[\text{Cu}(\text{pcp})(\text{bpy-ane}) \cdot 2.5\text{H}_2\text{O}]_n$ [where $\text{H}_2\text{pcp} = \text{P},\text{P}'$ -diphenylmethylenediphosphinic acid, $\text{bpy-ane} = 1,2$ -bis(4-pyridyl)ethane] displayed a very particular behavior: by heating the crystals up to 250°C , the water molecules were removed from the cavity but the framework remained unchanged.^{19,20} Above this temperature, the compounds started to decompose. On the contrary, when the crystal of MONT with bpy-ane was heated in water at 90°C for 30 days, the compound transformed into a 1D compound of formula $[\text{Cu}(\text{pcp})(\text{bpy-ane})(\text{H}_2\text{O})]_n$, a structural isomer without voids. In the same conditions, the analogous MONT with bipy remained unchanged. The reason of this behavior was attributed to the non-existence of a stable 1D phase for the latter due to a predicted thermodynamically unfavorable crystal packing.²¹ Herein, we report on the structural transformations observed in a novel class of nickel

phosphinates containing bipyridine co-ligands. By adding together Ni and pc₂p with the three co-ligands showed in chart 3, namely bipy, bpy-ane and 1,2-bis(4-pyridyl)ethylene (bpy-ene), we obtained 1D coordination polymers of general formula [Ni(H₂O)₄(bis-pyridine)·pc₂p]_n and with similar crystal arrangement constituted by cationic 1D chains of [Ni(H₂O)₄(bis-pyridine)]²⁺. The polymers with bpy-ane and bpy-ene maintain an ordered crystal arrangement after heating and they undergo a crystal-to-crystal transformation into a 3D coordination network. The study of these transformations sheds some light on the mechanism of network formation in different but related systems, such as the M(II), pc₂p, bis-pyridines and the M(II), pc₂p, bis-pyridines.

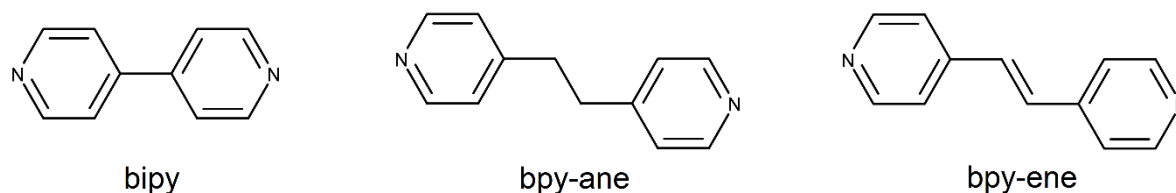


Chart 3. Structure of the nitrogenated co-ligands used in this work.

RESULTS AND DISCUSSION

Green crystals of [Ni(H₂O)₄(bipy)·pc₂p]_n (hereafter **1**), [Ni(H₂O)₄(bpy-ane)·pc₂p]_n (hereafter **2**) and [Ni(H₂O)₄(bpy-ene)·pc₂p]_n (hereafter **3**) were obtained by mixing in water nickel acetate, H₂pc₂p and bipy (**1**) or bpy-ane (**2**) or bpy-ene (**3**) at 90°C. Crystal structures of the three compounds were determined by single crystal X-ray diffraction analysis (Figure 1). All the structures are constituted of cationic 1D chains of [Ni(H₂O)₄(L)]_n²⁺ and dianionic diphosphate moieties. This arrangement, formed by a 1D string of metal, water and bis-pyridine intercalated by another anionic ligand, is relatively common in literature and most of the reported structures were obtained as side products in the attempt to synthesize 3D networks.²²⁻⁴⁴ The three compounds reported here are not isostructural and the space groups are different, as reported in table 1. The calculated density for **1** (1.547 g/dm³) is larger than those of **2** (1.421 g/dm³) and **3** (1.415 g/dm³).

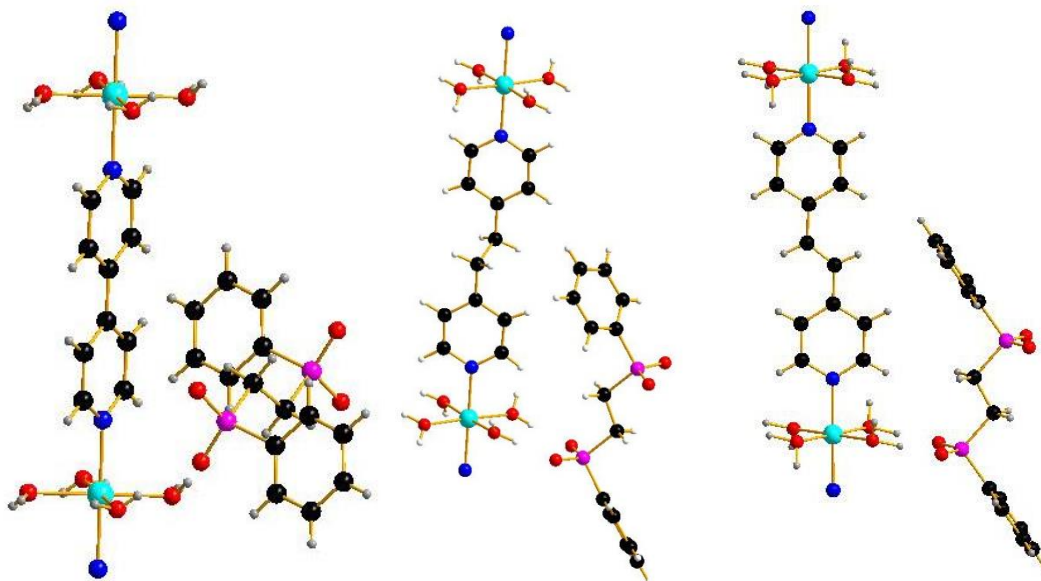


Figure 1. Fragment of the structures of **1** (left), **2** (center) and **3** (right).

Table 1. Crystal data and structure refinement for $[\text{Ni}(\text{H}_2\text{O})_4(\text{bipy})\cdot\text{pc}_2\text{p}]_n$, **1**, $[\text{Ni}(\text{H}_2\text{O})_4(\text{bpy-ane})\cdot\text{pc}_2\text{p}]_n$, **2**, $[\text{Ni}(\text{H}_2\text{O})_4(\text{bpy-ene})\cdot\text{pc}_2\text{p}]_n$, **3** and $[\text{Ni}(\text{H}_2\text{O})(\text{bpy-ene})(\text{pc}_2\text{p})]_n$, **3a**

Identification code	1	2	3	3a
Empirical formula	C ₂₄ H ₃₀ N ₂ Ni O ₈ P ₂	C ₂₆ H ₃₄ N ₂ Ni O ₈ P ₂	C ₂₆ H ₃₂ N ₂ Ni O ₈ P ₂	C ₅₂ H ₄₄ N ₄ Ni ₂ O ₁₀ P ₄
Formula weight	595.15	623.20	621.18	1126.21
Temperature (K)	293(2)	100(2)	173(2)	173(2)
Wavelength (Å)	0.71069	1.54184	0.71069	0.71069
Crystal System	Triclinic	Monoclinic	Monoclinic	Monoclinic
Space Group	P-1	C2/c	C2/m	C2/c
Unit Cell Dimensions (Å, °)	a=7.196 (1) b=9.841(3) c=10.381(2) α=63.70(2) β=75.86(2) γ=81.99(2)	a = 11.5588(3) b = 9.4672(2) c = 27.3181(6) β = 102.907(2)	a = 11.5550(9) b = 9.4320(9) c = 13.6180(10) β = 100.701(8)	a = 25.6156(8) b = 9.4288(3) c = 21.3284(8) β = 94.458(4)
Volume (Å ³)	638.7(3)	2913.9(1)	1458.4(2)	5135.7(3)
Z	1	4	2	4
Density (calculated) (g/cm ³)	1.547	1.421	1.415	1.457
Absorption coefficient (mm ⁻¹)	0.937	2.424	0.824	0.920
F(000)	310	1304	648	2320
Crystal size (mm)	0.570 x 0.100 x 0.100	0.2 x 0.1 x 0.08	0.45 x 0.15 x 0.15	0.2 x 0.2 x 0.15

Theta range for data collection (°)	2.236 to 24.970	6.093 to 72.262	4.369 to 28.890	4.265 to 29.328
Index ranges	0<=h<=8, -11<=k<=11, -11<=l<=12	-13<=h<=14, -11<=k<=8, -33<=l<=33	-11<=h<=15, -11<=k<=11, -18<=l<=17	-32<=h<=29, -12<=k<=9, -28<=l<=29
Reflections collected	2441	15787	3436	12104
Independent reflections	2246 [R(int) = 0.0231]	2858 [R(int) = 0.0464]	1775 [R(int) = 0.0462]	5871 [R(int) = 0.0356]
Completeness	96.4 % (to theta=25.240°)	99.8 % (to theta=67.684°)	98.9 % (to theta=25.000°)	98.8 % (to theta=25.240°)
Refinement method	Full-matrix least-squares on F ²	Full-matrix least-squares on F ²	Full-matrix least-squares on F ²	Full-matrix least-squares on F ²
Data / restraints / parameters	2246 / 0 / 185	2858 / 0 / 245	1775 / 0 / 107	5871 / 0 / 306
Goodness-of-fit on F ²	1.071	1.075	0.965	0.947
Final R indices [I>2sigma(I)]	R1 = 0.0290, wR2 = 0.0699	R1 = 0.0382, wR2 = 0.0874	R1 = 0.0446, wR2 = 0.0951	R1 = 0.0588, wR2 = 0.1568
R indices (all data)	R1 = 0.0397, wR2 = 0.0737	R1 = 0.0516, wR2 = 0.0952	R1 = 0.0756, wR2 = 0.1008	R1 = 0.0972, wR2 = 0.1703

In all cases, Ni(II) metal atom is octahedrally coordinated by four water molecules and by two nitrogen atoms belonging to two different bis-pyridine ligands. The Ni-O and Ni-N distances are comparable in the three compounds (see Table S1, ESI). The conformation of pc₂p can be defined using the C_{ipso}-P-P-C_{ipso} dihedral angle where C_{ipso} is the carbon atom of the phenyl ring bonded to the phosphorus atom. The value of the angle is about 180° for all the structures. This value is one of the most recurrent in the pc₂p complexes reported up to now.⁴⁵ Strong hydrogen bonds, with O-O distances in the range 2.64-2.76Å, exist between the water molecules and the oxygen atoms of the pc₂p. The Ni(H₂O)₄ groups are surrounded by four pc₂p anions and the oxygen atoms of the pc₂p are connected with four different Ni(H₂O)₄ moieties. The H-bond network in **1** is different with respect to **2** and **3**, as shown in Figure S1. Therefore, the whole supramolecular arrangement is different and it is schematically illustrated in Figure 2. The pc₂p group is represented by a purple cylinder while the [Ni(H₂O)₄(bis-pyridine)]_n column is schematized by a line formed by green cubes and light blue parallelepipeds. In **2** and **3**, the cylinders and the cubes are arranged as in a chessboard, while in **1** the pc₂p are intercalated between the lines of the [Ni(H₂O)₄(bis-pyridine)]_n columns.

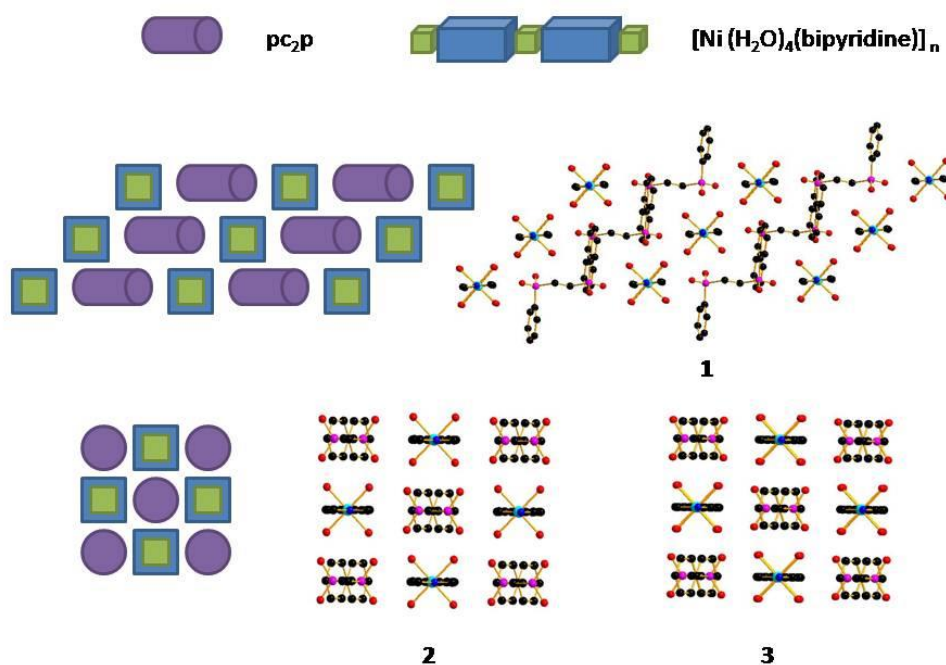
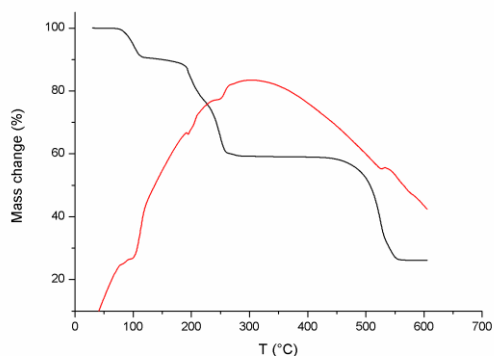


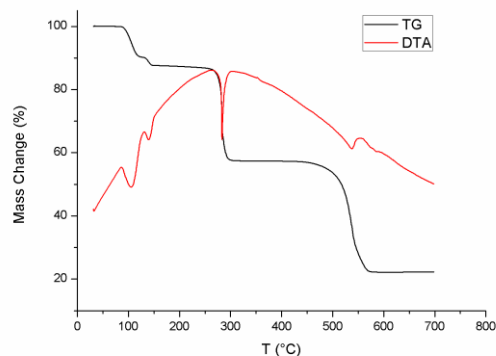
Figure 2. Schematic representation of the crystal packing for **1**, **2** and **3**. Purple cylinders represent pc_{2p} groups; green cubes ($Ni(H_2O)_4$) and light blue parallelepipeds (bis-pyridine) are used to visualize the $[Ni(H_2O)_4(\text{bis-pyridine})]_n$ columns.

We expected that crystal structures **1-3** were good candidates for solid state transformations driven by temperature. The phosphinate moiety decomposes at around 300°C , a temperature comparable to thermally stable carboxylate based MOFs. We have also previously observed that the coordination polymers formed by bis-pyridines and phosphinates are generally crystalline and stable up to the decomposition temperature of bis-pyridines (250°C).¹²⁻¹⁷ Thermogravimetric analysis (TGA) of **1** shows that the phase is stable up to 150°C (see Figure S2). The observed weight loss of 37.6% (35.8 Calcd.) corresponds to the release of the four water molecules and the degradation of the bipy. Between 270°C and 450°C , the diagram shows a new stability range that most likely corresponds to $[Ni(pc_{2p})]_n$ phase. The temperature dependent X-ray diffraction (TD-XRD) experiment (see Figure S3) shows that **1** is stable and crystalline up to 150°C . At higher temperature, only few broad peaks are observed and they are attributed to the $[Ni(pc_{2p})]_n$ phase. In the case of **2**, as shown in Figure 3a, the synthesized phase is stable up to 90°C . The weight loss between 90°C and 140°C corresponds to the removal of four water molecules (exp. 11.0%, calcd 11.6%). The successive loss corresponds to the burning of the bis-pyridine ligand (exp. 39.2; calcd. 41.1). The TD-XRD analysis between room temperature and 100°C (see Figure 3c) confirms the results of the TGA, i.e. the anhydrous $[Ni(\text{bpy-ene})(pc_{2p})]_n$ phase, **2b**, is a crystalline

phase. In addition, it is relatively stable at room temperature, as additional peaks of the pristine compound are only seen after 17 hours in ambient conditions. Such behavior allowed us to readily stabilize **2b** to collect high-resolution powder X-ray diffraction (PXRD) data at 110 °C. Powder pattern indexing led to unit cell dimensions close to their precursor's, *i.e.*, $a = 10.656(8) \text{ \AA}$, $b = 12.941(8) \text{ \AA}$, $c = 26.22(1) \text{ \AA}$, $\beta = 94.52(6)^\circ$, $V = 3604.8 \text{ \AA}^3$ [$M_{17} = 11.2$, $F_{17} = 27(0.107, 60)$], probable space group $P2/m$. This result suggests that the full dehydration does not modify drastically the crystal structure of **2**, and the schematic arrangement of entities could obviously be preserved as illustrated in Figure 2. More on the possible structure of **2b** will be discussed below. The TGA of **3** is reported in Figure 3b. There is no significant weight loss up to 90°C. In the range 90°C – 120°C, the corresponding weight losses match with the removal of three water molecules (exp. 8.9%, Calcd 8.7%). Between 140°C and 160°C, also the fourth water molecule is lost (exp. 2.7%, Calcd 2.9%). The anhydrous phase is stable up to 200°C. The additional weight loss corresponds to the removal of the bipyridine at higher temperature. Finally, the $[\text{Ni}(\text{pc}_2\text{p})]_n$ phase is stable up to 450°C. A TD-XRD experiment, performed at a much lower heating rate up to 160 °C, allowed to observe the corresponding dehydration stages at lower temperatures, as shown in figure 3d. The $[\text{Ni}(\text{H}_2\text{O})(\text{bpy-ene})(\text{pc}_2\text{p})]_n$ phase, **3a**, is obtained as a crystalline phase between 60 and 100 °C. It transforms into the crystalline anhydrous $[\text{Ni}(\text{bpy-ene})(\text{pc}_2\text{p})]_n$ phase, **3b**, which is observed till the end of the experiment at 160 °C. In this case *ab-initio* indexing was not possible due to loss of crystallinity and broadening of many peaks. An additional *in situ* XRD experiment was performed while cooling the sample in different atmospheres, to evaluate whether **3b** is stable in ambient conditions. This phase seems only sensitive to water, as it rehydrates into its monohydrate parent **3a** in air, while it is stable under pure N₂ (see Figure S3). Additionally, phase **3a** does not convert back into **3** when placed in contact with water.



(a)



(b)

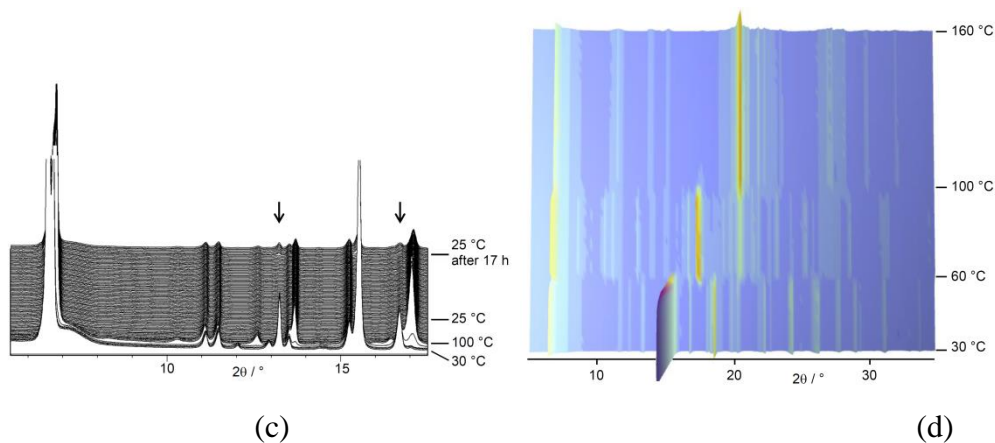


Figure 3: (a) TG/DTA curve of compound **2**; (b) TG/DTA curve of compound **3**; (c) temperature dependent XRD experiment showing the dehydration of **2** and the slow re-hydration of **2b** back to ambient (d); temperature dependent XRD experiment for **3**.

We tried to dehydrate single crystals of **2** and **3** simply by heating a batch of crystals at 140 °C for one night under vacuum. For **2**, we did not obtain suitable crystals, while for **3** after the treatment, it was possible to collect and solve the structure of **3a** by single crystal X-ray diffraction. As already pointed out, in air **3b** spontaneously rehydrates into its monohydrate parent.

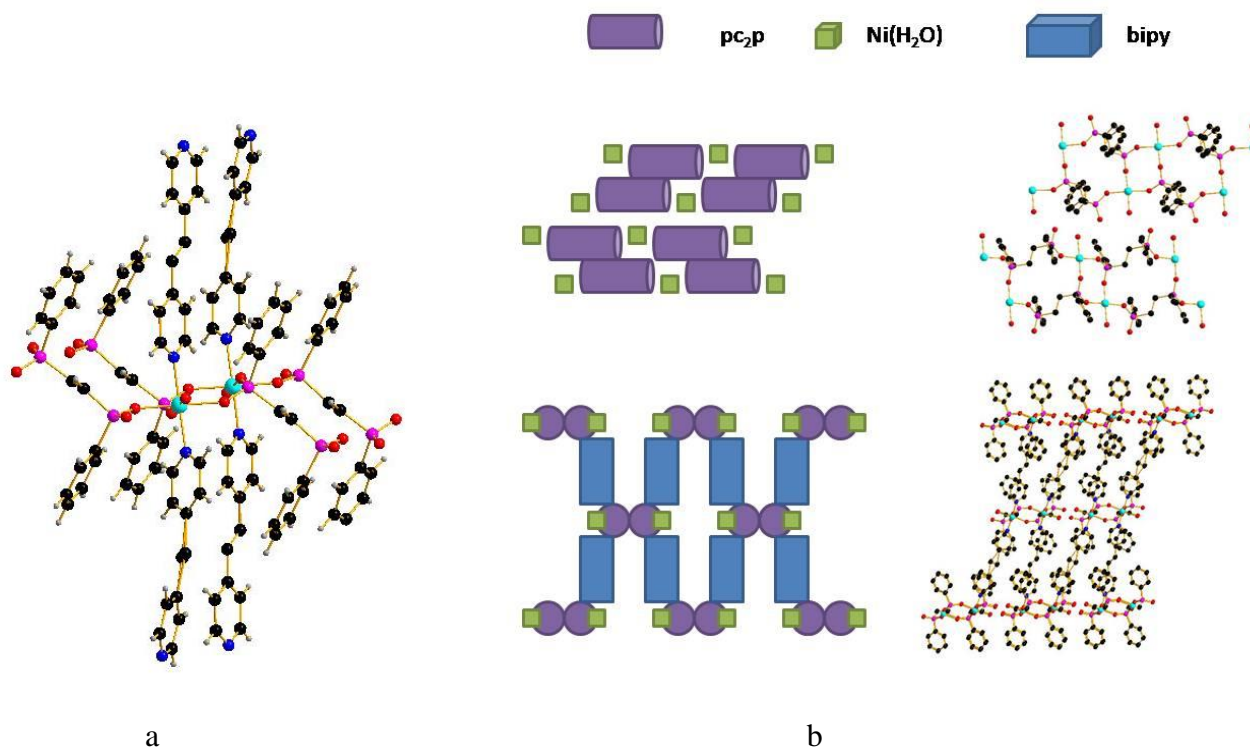


Figure 4. a) Fragment of the structures of **3a** b) Crystal packing of **3a**. In this case, the green square represents the Nickel atom bonded to one water molecule.

In order to schematize the network, the same representation of Figure 2 for pc₂p, bipy and Ni(H₂O) was used, as well as the corresponding stick and ball models (hydrogen atoms are omitted). The 3D network of **3a** is assembled using Ni and pc₂p (phenyl rings are omitted) in 1D sheets; the latter are connected by the bipyridine molecule. Ni(II) is still octahedrally coordinated, but three basal coordination sites are hereby occupied by oxygen atoms of three different pc₂p ligands and the fourth position is taken up by a water molecule (Figure 4a). The 1D pillars of [Ni(bipy)] are now connected by the pc₂p ligand. A new 1D [Ni(H₂O)(pc₂p)] chain is formed, as shown in Figure 4b. Strong hydrogen bonds are formed between the water molecules and the oxygen atoms of the diphosphate groups not involved in the metal coordination (O-O distances = 2.71 Å). The 1D [Ni(bpy-ene)] pillars connect the 1D [Nipc₂p] chains and the resulting structure is a 3D network with 3-connected (pc₂p ligand) and 5-connected (Nickel atom) nodes. Figure 5 shows the proposed mechanism of formation of **3a**, focusing on the breaking and formation of coordination bonds that involve Ni and pc₂p, modeled upon the crystal structure of **3**: removal of three water molecules from the Ni coordination sphere (Figure 5a to 5b) triggers reorganization of the hydrogen bonds network and every pc₂p molecule coordinates to three different Ni atoms (Figure 5b to 5c), thus leading to twisting of the pc₂p units and formation of the chains of Ni(pc₂p) held together by hydrogen bonds observed in **3a** (Figure 5c to 5d).

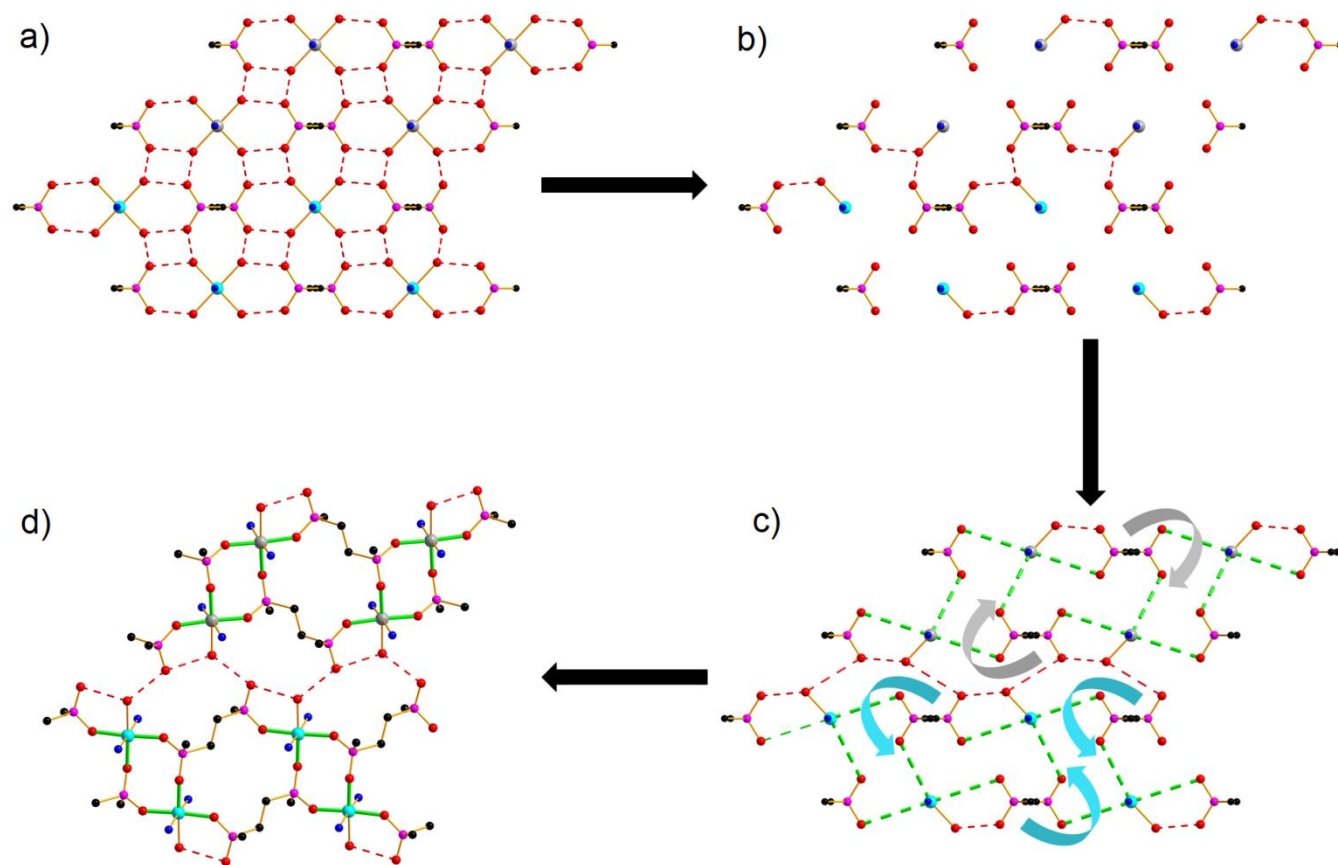


Figure 5. Proposed mechanism for the phase transition leading from **3** to **3a**. (a) Arrangement of Ni

octahedra and pc₂p units in **3**. (b) Residual coordination bonds and hydrogen bonds in **3** after removal of three water molecules per Ni atom. (c) Reorganization of hydrogen bonds and formation of new coordination bonds between pc₂p units and Ni atoms, accompanied by twisting of the pc₂p. (d) Final structure of **3a**. Different colors are used to distinguish Ni atoms that end up belonging to different chains in **3a**. Colour code: Ni atoms are represented in light blue and light gray, P atoms are represented in pink, C atoms are represented in black, O atoms are represented in red, N atoms are represented in blue, H atoms are represented in white. Hydrogen bonds are represented as red dashed lines. Newly formed coordination bonds are represented as dashed green lines in (c) and bold green lines in (d).

Substantial reorganization of the π - π stacking interactions network takes place during the phase transition (Figure S4). **1**, **2** and **3** all feature similar π - π stacking interactions between the phenyl rings of adjacent pc₂p units, while bis-pyridines are not involved in any non-covalent interaction. In **3a** this arrangement is disrupted and new interactions involving also bpy-ene are established. The phase transition does not involve breaking and formation of bonds between bpy-ene and Ni, however the [Ni(bpy-ene)] chains experience a significant distortion in **3a** (Figure S5). The topological analysis reveals a 3,5T1 net, reported to be in the first 30 most frequent underline single net.⁴² Considering the hydrogen bond between the uncoordinated oxygen atom of diphosphate and the water molecule, the overall topology becomes fsc with a 4-connected (pc₂p ligand) and 6-connected (Nickel atom) nodes. This gives us some hints on the structure **3b**. Likely, the uncoordinated oxygen atoms of the phosphinic ligands could displace the coordinated water molecule thus connecting to the Nickel atom and extending the connectivity into a 3D network.

We have presented a very special case in which quasi-similar CPs behave in very different ways, under the same heating conditions. To summarize, at first glance **1**, **2** and **3** are almost the same compounds, having the same formula, the same coordination environment around the Ni metal atom and forming the same 1D network. A closer look reveals a different supramolecular arrangement for **1**, **2** and **3** as well as a different calculated density. The change in behavior could be ascribed to the different length of the bridging unit of the two pyridine molecules. The N-N distances are 7.112(3), 9.390(2) and 9.436(4) Å for bipy, bpy-ane and bpy-ene in **1**, **2**, and **3**, respectively. The two latter values have to be compared with the equivalent distances of phosphorus atoms of two pc₂p in **2** and **3**, i.e., 9.799(2) Å and 9.855(2) Å respectively. With this in mind, bipy is clearly too short to allow the crystal arrangement shown by **3a** or the expected one for **2b** and **3b**. The identification of the partially hydrated phase **3a** could be related to the different flexibility of bpy-ane and bpy-ene. Bpy-ene preferably adopts a planar conformation, owing to the conjugation of the two pyridine rings through the double bond. In **3a**, one of the

crystallographically independent bpy-ene units is already significantly distorted and it is likely that **3b** demands even more distortion. This suggests that the system prefers to retain one water molecule coordinated to each Ni atom instead than replacing it with a P-O group from a phosphinate unit. As a matter of fact, **3b** readily uptakes one water molecule when exposed to moist air, while **3a** is stable over a long period in the presence of water. In the case of **2**, the ideal monohydrate phase **2a** was probably not isolated because the higher flexibility of bpy-ane molecule leads to preferential stabilization of compound **2b**.

These findings help us to critically review other transformations observed in previous papers such as the transformation of the 1D MONT compound in 1D strip.²⁰ In that example, the phosphinic ligand (pcp) was linked to copper forming [Cu(pcp)]_n 1D columns. These columns remained stable during the transformation while Cu-N bonds were broken and reformed. In the present work, we observed that the [Ni(bis-pyridine)]_n columns remained the same while new Ni-O bonds were formed in the process. This behavior could be related both to the different strength of the metal-ligand bonds in the two series of compound but also the better chelating ability of pcp, compared to pc₂p, could have a certain importance in the building up well stable [Cu(pcp)]_n columns.

Conclusions

In this paper, the structure and reactivity of three related 1D Ni-phosphinate CPs were studied. For the three compounds, we have reported how the transformation of 1D coordination compounds in 3D ones induced by the temperature took place. The different mechanisms involved in the formation of the 3D coordination polymers in the case of two related class of ligand which differ only by a methylene group (namely the pcp and the pc₂p ligands) were discussed. We found that pcp reacts first with the metallic center and after the formation of a corner-like polymer the connection among the bipys occurred. In the case of pc₂p, we have found that the affinity of the latter ligand is lower than the one of the bipys. In this way, infinite 1D chains formed by [M(bipy)]_n are present in solution and the pc₂p connect them to build the tridimensional structures. We can say that structures **1**, **2** and **3** can be considered a sort of proto-coordination polymers able to afford novel 3D structures upon heating which cannot be obtained by direct synthesis. In our opinion, this study added important features to the comprehension of the chemistry of CPs based on transition metal phosphinates.

Experimental Section

Materials and Methods: All reagents were analytical-grade commercial products and were used without further purification. The p,p' - diphenylmethylenediphosphinic acid (H₂pcp) was prepared as previously described.^{47,48} Elemental analyses (C, H) were performed with an EA 1108 CHNS-O automatic analyzer. Coupled thermogravimetric (TG) and differential thermal analysis (DTA) measurements were performed using a Netzsch STA490C thermoanalyzer under a 20 mL min⁻¹ air flux with a heating rate of 10 C min⁻¹. *In situ* X-ray powder diffraction measurements were performed within an Anton Paar HTK 1200N chamber attached to a Panalytical Empyrean powder diffractometer. (θ - θ Bragg-Brentano geometry) working with the Cu-K α radiation (λ K α_1 = 1.5406 Å, λ K α_2 = 1.5444 Å) selected with a flat multilayer X-ray mirror (Bragg-Brentano HD[®]). Data were collected with a Pixel 1D silicon-strip detector, in the useful angular range. Powder pattern indexing was carried out with the program DICVOL06.⁴⁹

Synthesis of [Ni(H₂O)₄(bipy)·pc₂p]_n,1: A solution of Ni(CH₃COO)₂·4H₂O (35 mg, 0.14mmol) in water (10 ml) was added to a boiling water solution (60ml) of H₂pc₂p (43 mg, 0.14mmol) and bipy (22 mg, 0.14mmol). The resulting solution was boiled till green cubes started separating. Then the mixture was held at ca. 80°C to complete the precipitation of the complex. The compound was filtered, washed with water and dried in air, at room temperature. Yield 68% based on Nickel. Anal. Calc. for C₂₄ H₃₀ Ni O₈ N₂ P₂, mw=595.15gmol⁻¹: C, 48.44; N, 4.71 ;H, 5.08. Found: C, 48.42; N, 4.69; H, 5.15%.

Synthesis of [Ni(H₂O)₄(bpy-ane)·pc₂p]_n,2: A solution of Ni(CH₃COO)₂·4H₂O (35 mg, 0.14mmol) in water (10 ml) was added to a boiling water solution (60ml) of H₂pc₂p (43 mg, 0.14 mmol) and bpy-ane (26 mg, 0.14mmol). The resulting solution was boiled till green cubes started separating. Then the mixture was held at ca. 80°C to complete the precipitation of the complex. The compound was filtered, washed with water and dried in air, at room temperature. Yield 74% based on Nickel. Anal. Calc. for C₂₆ H₃₄ Ni O₈ N₂ P₂, mw=623.20gmol⁻¹: C, 50.11; N, 4.50 ; H, 5.50. Found: C, 50.15; N, 4.45; H, 5.57%.

Synthesis of [Ni(H₂O)₄(bpy-ene)·pc₂p]_n,3: A solution of Ni(CH₃COO)₂·4H₂O (35 mg, 0.14mmol) in water (10 ml) was added to a boiling water solution (60ml) of H₂pc₂p (43 mg, 0.14mmol) and bpy-ene (26 mg, 0.14mmol). The resulting solution was boiled till green cubes started separating. Then the mixture was held at ca. 80°C to complete the precipitation of the complex. The compound was filtered, washed with water and dried in air, at room temperature. Yield 63% based on Nickel. Anal. Calc. for C₂₆ H₃₂ Ni O₈ N₂ P₂, mw=621.19gmol⁻¹: C, 50.27; N, 4.51 ; H, 5.19. Found: C, 50.30; N, 4.55; H, 5.28%.

X-Ray Structure Determination: The crystal data of compounds **1**, **2**, **3** and **3a** are presented in Table 1. The single-crystal X-ray experiments were carried out on a CCD diffractometer with Mo K α or Cu K α radiation. The program CrysAlisCCD⁵⁰ was used for data collection. Data reductions (including absorption corrections) were carried out with the program CrysAlis RED.⁵¹ The atomic coordinates were

obtained by the direct methods in Sir97.⁵² Structure refinements were performed with SHELXL⁵³ using the full-matrix least-squares method for all the available F² data. All the non-hydrogen atoms were refined anisotropically.

ACKNOWLEDGEMENTS

A.I. and T.B. are grateful for the Short Term Mobility Program 2013. M.T. is supported by funding from the European Union's Horizon 2020 research and innovation program under the Marie Skłodowska-Curie grant agreement No 663830. AI acknowledges Mr. Carlo Bartoli for his technical assistance.

AUTHOR INFORMATION

E-mail:

Ferdinando Costantino ferdinando.costantino@unipg.it,

Andrea Ienco andrea.ienco@iccom.cnr.it

Note: The authors declare no competing financial interest.

ASSOCIATED CONTENT

CCDC 1564548-1564551 contain the supplementary crystallographic data for this paper. These data can be obtained free of charge via www.ccdc.cam.ac.uk/data_request/cif, or by emailing data_request@ccdc.cam.ac.uk, or by contacting The Cambridge Crystallographic Data Centre, 12 Union Road, Cambridge CB2 1EZ, UK; fax: +44 1223 336033.

Supporting information available

The supporting information is available free of charge on the ACS publication website at: DOI xxxx
Crystallographic tables containing structural information, bond lengths and angles for compounds **1**, **2**, **3** and **3a**. TGA analysis for compound **1**. Temperature dependent XRPD patterns for compound **1**. Additional structural figures showing the H-bonds nets and the $\pi - \pi$ stacking for compounds **2** and **3**. IR and UV-VIS spectra are also reported.

REFERENCES

- (1) V. V. Boldyrev, *Reactivity of Solids: Past, Present and Future*, Blackwell Science, Cambridge, **1996**.
- (2) Vittal, J. J.; *Coord. Chem. Rev.* **2007**, *251*, 1781-1795.
- (3) Kole, G. K.; Vittal, J. J. *Chem. Soc. Rev.* **2013**, *42*, 1755-1775.
- (4) Li, C.-P.; Chen, J.; Liu, C.-S.; Du, M. *Chem. Commun.* **2015**, *51*, 2768-2781.
- (5) Tanaka, K. and Toda, F. *Chem. Rev.* **2000**, *100*, 1025-1074.
- (6) Rather B. and Zaworotko, M. J. *Chem. Commun.* **2003**, 830-831.
- (7) Sun, H.-L., Yin, D.-D.; Chen, Q., Wang, Z. *Inorg. Chem.* **2013**, *52*, 3582-3584
- (8) Zhang, J.-P.; Lin, Y.-Y.; Zhang, W.-X.; Chen, X.-M. *J. Am. Chem. Soc.* **2005**, *127*, 14162-14163
- (9) Férey, G. and Serre, C. *Chem. Soc. Rev.* **2009**, *38*, 1380-1399.
- (10) Habib, H. A.; Sanchiz, J.; Janiak, C. *Dalton Trans.* **2008**, 1734-1744.
- (11) Volkringer, C.; Loiseau, T.; Guillou, N.; Férey, G.; Elkaïm, E.; Vimont, A. *Dalton Trans.* **2009**, 2241-2249.
- (12) Taddei, M.; Costantino, F.; Ienco, A.; Comotti, A.; Dau, P. V.; Cohen, S. M. *Chem. Commun.* **2013**, *49*, 1315-1317.

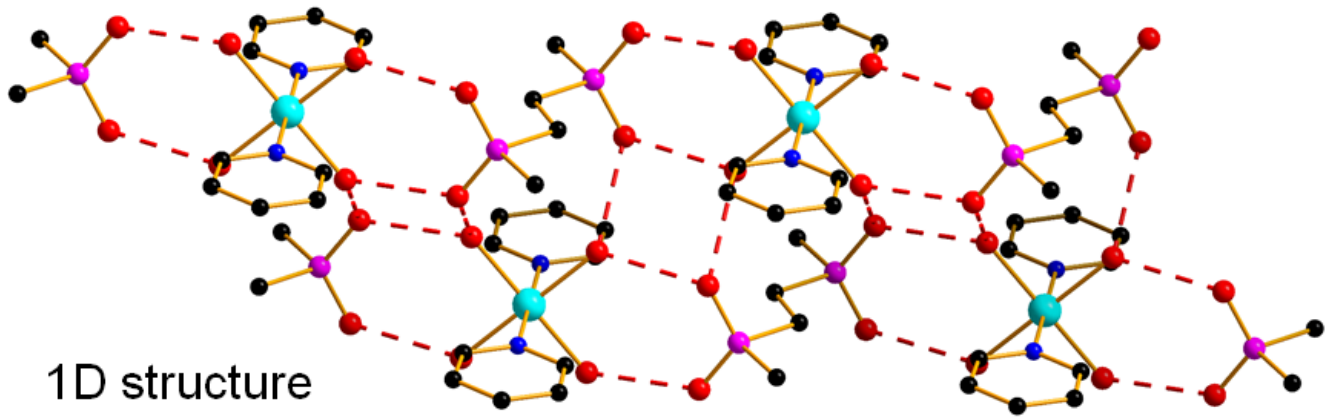
- (13) J.-P. Zhang , P.-Q. Liao , H.-L. Zhou , R.-B. Lin, X.-M. Chen *Chem. Soc. Rev.*, **2014**, *43*, 5789-5814; J. Sánchez Costa, S. Rodríguez-Jiménez, G. A. Craig, B. Barth, C. M. Beavers, S. J. Teat, G. Aromí *Journal of the American Chemical Society* **2014** *136*, 3869-3874; E. Lee, Y. Kim, J. Heo, and K.-M Park *Cryst. Growth Des.* **2015** *15*, 3556-3560; X.-P. Wang , W.-M Chen, H. Qi, X.-Y Li, C. Rajnák, Z.-Y Feng, M. Kurmoo, R. Boča, C.-J. Jia, C.-H. Tung, D. Sun, *Chemistry - A European Journal* **2017**, *23*, 7990-7996; L. -H Cao, Y. -S Wei, H. Xu, S. -Q Zang, T. C. W. Mak. *Advanced Functional Materials* **2015**, *25*, 6448-6457.
- (14) Costantino, F.; Ienco, A.; Taddei, M. Tailored Organic-Inorganic Materials (Eds.: E. Brunet, J. L. Colon, A. Clearfield), John Wiley & Sons, **2015**, 193–244; Costantino, F.; Ienco, A.; Taddei, M. Non-covalent Interactions in the Synthesis and Design of New Compounds (Eds.: Maharramov, A. M.; Mahmudov, K. T.; Kopylovich, M. N.; Pombeiro, A.J.L.) John Wiley & Sons, **2016**, 163-184.
- (15) Vioux, A.; Le Bideau, J.; Mutin, P. H.; Leclercq, D. Topics in Current Chemistry, Springer-Verlag, Heidelberg, **2004**, 145.
- (16) Carson, I., Healy, M.R., Doidge, E.D., Love, J.B., Morrison, C.A., Tasker, P.A. *Coord. Chem. Rev.* **2017**, *335*, 150-171.
- (17) Bataille, T.; Costantino, F.; Ienco, A.; Guerri, A.; Marmottini, F.; Midollini, S. *Chem. Commun.* **2008**, 6381-6383.
- (18) Costantino, F.; Ienco, A.; Midollini, S. *Cryst. Growth Des.* **2010**, *10*, 7-10.
- (19) Bataille, T.; Costantino, F.; Lorenzo-Luis, P.; Midollini, S.; Orlandini, A. *Inorg. Chim. Acta* **2008**, *361*, 327-334.
- (20) Bataille, T.; Bracco, S.; Comotti, A.; Costantino, F.; Guerri, A.; Ienco, A.; Marmottini, F. *CrystEngComm* **2012**, *14*, 7170-7173.
- (21) Taddei, M.; Ienco, A.; Costantino, F.; Guerri, A. *RSC Adv* **2013**, *3*, 26177-26183.
- (22) Woodward, J.D.; Backov, R.V.; Abboud, K.A.; Talham, D.R. *Polyhedron* **2006**, *25*, 2605-2615.
- (23) Marinescu, G.; Andruh, M.; Julve, M.; Lloret, F.; Llusar, R.; Uriel, S.; Vaissermann, J. *Cryst. Growth Des.* **2005**, *5*, 261-267.
- (24) Wang, R.; Jiang, F.; Zhou, Y.; Han, L.; Hong, M. *Inorg. Chim. Acta* **2005**, *358*, 545-545.
- (25) Chen, H.-Ji; Huaxue, H. *Jiegou Huaxue (Chin. J. Struct. Chem.)* **2005**, *24*, 236-240.
- (26) Zhang, L-P.; Zhu, L-G. *Acta Crystallogr. Sect. E: Struct. Rep. Online* **2005**, *E61*, m1768-m1770.
- (27) Dong, H-L; Xu, L.; Liu, Q-Y.; R-L. Sang *Acta Crystallogr. Sect. E: Struct. Rep. Online* **2005**, *E61*, m2340-m2342.
- (28) Gao, J-S.; Hou, G-F.; Yu, Y-H.; Hou, Y-J.; Yan, P-F. *Acta Crystallogr. Sect. E: Struct. Rep. Online* **2006**, *E62*, m2913-m2915.
- (29) Chen, Z.; Liang, F.; Tang, X.; Chen, M.; Song, L.; Hu, R.Z. *Anorg. Allg. Chem.* **2005**, *631*, 3092-3095.

- (30) Liu, Y.; Dou, J-M.; Wang, D-Q.; Li, D-C.; Xu, F.; Zhou, L.; Su, H-J. *Jiegou Huaxue (Chin. J. Struct. Chem.)* **2006**, 25, 895-902.
- (31) Tong, M-L.; Lee, H. K.; Chen, X-M.; Huang, R-B.; Mak, T.C.W. *J. Chem. Soc. Dalton Trans.* **1999**, 3657-3659.
- (32) Lei, C.; Mao, J-G.; Sun, Y-Q.; Dong, Z-C. *Polyhedron* **2005**, 24, 295-303.
- (33) Wei, Y-H.; Tan, A-Z.; Chen, Z-L.; Liang, F-P.; Hu, R-X. *Chin. J. Inorg. Chem.* **2006**, 22, 273-280
- (34) Huo, X-K.; Ma, L-F.; Wang, L-Y.; Fan, Y-T. *Chin. J. Inorg. Chem.* **2007**, 23, 401-406.
- (35) Zhang, L-P.; Zhu, L-G. *CrystEngComm* **2006**, 8, 815-826.
- (36) Lu, S-F.; Zhu, Y-B.; Liang, Y-C.; Yu, R-M.; Huang, X-Y.; Sun, F-X. Wu, Q-J.; Huang, Z-X. *Acta Chim. Sinica* **2004**, 62, 253-261.
- (37) Wang, X-L.; Qin, C.; Wang, E-B. *Cryst. Growth Des.* **2006**, 6, 439-443
- (38) Tao, J.; Huang, R-B.; Zheng, L-S.; S.W. Ng *Acta Crystallogr., Sect. E: Struct. Rep. Online* **2003**, E59, m614-m615.
- (39) Paz, F. A. A.; Khimiyak, Y.Z.; Klinowski, J. *Acta Crystallogr., Sect. E: Struct. Rep. Online* **2003**, E59, m8-m10.
- (40) Wang, Q-W.; Li, X-M.; Han, J. *Jiegou Huaxue (Chin. J. Struct. Chem.)* **2006**, 25, 1369-1374
- (41) Zhou, Q-X.; Xu, Q-F.; Lu, J-M.; Xia, X-W. *Jiegou Huaxue (Chin. J. Struct. Chem.)* **2006**, 25, 1392 – 1396.
- (42) Zhang, L-P.; Zhu, L-G. *Acta Crystallogr., Sect. E: Struct. Rep. Online* **2005**, E61, m1264-m1265
- (43) Xie, H-Z.; Li, Z-F.; Zheng, Y-Q. *Acta Crystallogr., Sect. C: Cryst. Struct. Commun.* **2007**, 63, m30-m32.
- (44) Williams, P.A.M.; Ferrer, E.G.; Baran, E.J.; Piro, O.E.; Ellena, J.A.; Castellano, E.E. *CCDC 188089: Experimental Crystal Structure Determination* **2014**, doi: 10.5517/cc69qdl.
- (45) Costantino, F.; Ienco, A.; Midollini, S.; Orlandini, A.; Sorace, L.; Vacca, A. *Eur J. Inorg. Chem.* **2008**, 3046-3055.
- (46) Alexandrov, E. V., Blatov, V. A., Kochetkov, A. V; Proserpio, D. M. *CrystEngComm* **2008**, 13, 3947-3958.
- (47) Midollini, S.; Lorenzo-Luis, P.; Orlandini, A. *Inorg. Chim. Acta* **2006**, 359, 3275-3282
- (48) Garst, M.E. *Synth. Commun.*, **1979**, 9, 261-266.
- (49) Boultif, A; Louër, D. *J. Appl. Crystallogr.* **2004**, 37, 724-731.
- (50) CrysAlisCCD, Oxford Diffraction Ltd., Version 1.171.33.41 (release 06-05-2009 CrysAlis171.NET)
- (51) CrysAlisRED, Oxford Diffraction Ltd., Version 1.171.33.41 (release 06-05-2009 CrysAlis171.NET)
- (52) Altomare, A.; Burla, M.C.; Cavalli, M.; Cascarano, G.L.; Giacovazzo, C.; Gagliardi, A.; Moliterni,


A.G.G.; Polidori, G.; Spagna, R. *J.Appl.Crystallogr.* **1999**, 32,115-119.

(53) Sheldrick, G. M. *Acta Crystallogr.* **2008**, A64, 112-122.

TABLE OF CONTENT GRAPHICS



Water removal



A large black arrow pointing downwards, indicating the process of water removal from the 1D structure to the 3D structure.

